

Impact of the acrylic vessel on the light collection

E. Bonvin
CRL, Chalk River

June 17, 1991

1 Introduction

As suggested by Zwinkels, Davidson and Dodd (SNO-89-11), the optical properties of acrylic depend on the manufacturer, the fabrication and the aging history. This report aims to quantify the overall light collection in SNO for different types and thicknesses of acrylic. It also identifies light losses occurring for vertices located near the acrylic vessel. These losses are specially significant for a thicker vessel and might indirectly magnify the low energy H_2O background.

2 Figure of Merit for light transmission

To quantitatively compare the optical properties of different types and thicknesses of acrylic in a frame relevant to SNO, a computer program has been written. It folds together the Čerenkov spectrum emitted at random angles from randomly distributed vertices inside the D_2O with the light transmissions through the D_2O , the acrylic and the H_2O and the PMT quantum efficiency. The water absorption coefficients are as reported in the white book SNO-87-12, the quantum efficiency is as provided by Queen's for Tube R1408, Serial # ZW535, and the acrylic coefficients are as measured at NRC by Zwinkels et al., SNO-89-11 (from Fig. 8 for thermoformed, aged Rohm acrylic, from Fig. 9 for thermoformed, aged Polycast acrylic). The program does not take into account partial reflection at the different material interfaces (water-acrylic, water-glass), light scattering effects or soft reflection on the PMTs reflectors. Fig. 1. shows, as a function of the wavelength, three light spectra for different assumptions. The full line curve shows the PMT response to Čerenkov light without light absorption in D_2O , H_2O or acrylic; the spectrum has a maximum around 320 nm. When the absorptions in D_2O and H_2O are considered (dotted line) the total detectable light diminishes by 25% and the spectrum is slightly shifted towards longer wavelengths (max. at 330 nm). When the absorption in acrylic is also taken into account (dashed curve), the shortest wavelengths are strongly suppressed due to the UV cut-off of acrylic around 340 nm, an additional

thickness	Rohm	Polycast
1"	0.79	0.73
2"	0.69	0.62
3"	0.62	0.58
4"	0.57	0.54

Table 1: Figure of merit for different acrylic thicknesses

36% of the light is lost (for 2" thick Polycast acrylic) and the final light spectrum has its maximum around 380 nm. The figure of merit of a given type of acrylic is then defined as

$$F = \frac{\sum_{\lambda} C \cdot T_{D_2O} \cdot T_{acry} \cdot T_{H_2O} \cdot Q_{PMT}}{\sum_{\lambda} C \cdot T_{D_2O} \cdot T_{H_2O} \cdot Q_{PMT}} \quad (1)$$

where C is the Čerenkov spectrum, T_{D_2O} , T_{H_2O} and T_{acry} are respectively the light transmission through the D_2O , the H_2O and the acrylic and Q_{PMT} is the phototube quantum efficiency. Table 1. gives the figures of merit of thermoformed, aged acrylic, for different thicknesses. The Rohm sample measured at NRC is better than the Polycast sample. A 1" thick vessel under tension would mean 18% more detectable light than a vessel under compression as in the present design (2" thick, with a 3" thick half dome and a 4" thick waist) . More data on different samples and over the whole relevant spectral window (250 nm to 600 nm) are however required before drawing definitive conclusions.

3 Events near the vessel

As the event vertex moves away from the center of the vessel, the average distance travelled by photons through the acrylic increases and peaks for vertices adjacent to the vessel wall as shown in Fig. 2 for a 2" thick vessel. Therefore the light absorption also increases and events occurring near the vessel ($r \approx 5.5 - 6$ m) produce less detectable light than events near the center of the D_2O . This loss could rather easily be measured in the detector by calibration sources: However more significant is the fact that vertices generated in the H_2O produce more detectable light than events in the D_2O , since most of the light is no longer attenuated by the acrylic. Fig. 3 shows the amount of detectable light as a function of the vertex position along the radius. For a 2" thick Rohm acrylic vessel, the drop from center to near the vessel is around 12% whereas the D_2O - H_2O step is a 30% effect. This D_2O - H_2O step is more significant as a consequence of the extremely good UV-response of the new Hamamatsu PMT, as compared to those of earlier prototypes (Fig.1 to be compared with Fig. 3.2 in the White Book).

As shown in Fig. 4, this local effect is even more pronounced when the detectable light is plotted (for a given r) as a function of $\cos(\theta)$, where θ is the angle between the radius and the ray of light. For H_2O events (at $r = 6.05$ m), the sharp drop for angles with $\cos(\theta) \approx 0.2$ is a consequence of the light crossing obliquely two

thicknesses of acrylic and therefore being strongly attenuated. For those angles with $\cos\theta \leq 0.1$ the light generated in the H_2O doesn't cross the acrylic wall, and the ratio of the detectable light from the H_2O (at $r = 6.05\text{m}$) to that from the D_2O (at $r = 5.9\text{ m}$) is respectively 1.9, 2.5, 3.0 and 3.6 for 1", 2", 3" and 4" thick vessel. Since the position resolution in SNO is expected to be about 25 cm, low energy ($\approx 2.5\text{ MeV}$ for a 2" thick vessel or $\approx 1.7\text{ MeV}$ for a 4" thick vessel) H_2O background could easily be reconstructed as higher energy (6 MeV) events in the D_2O .

Since 30% of the D_2O mass is within 50 cm of the vessel, no fiducial cut is desirable for CC events. The H_2O background increases sharply with decreasing energy and therefore a precise study of this background is desirable, specially since recent acrylic vessel designs tend to favor a thicker vessel. Moreover the program used is uniquely a ray-tracing code and doesn't consider non-linear Čerenkov emission at low energies nor multiple scattering and doesn't generate Čerenkov cones, all effects that might average the angular distribution of the detectable light. Therefore a complete and more accurate study with the standard SNO Monte-Carlo is needed to fully appreciate the described effects.

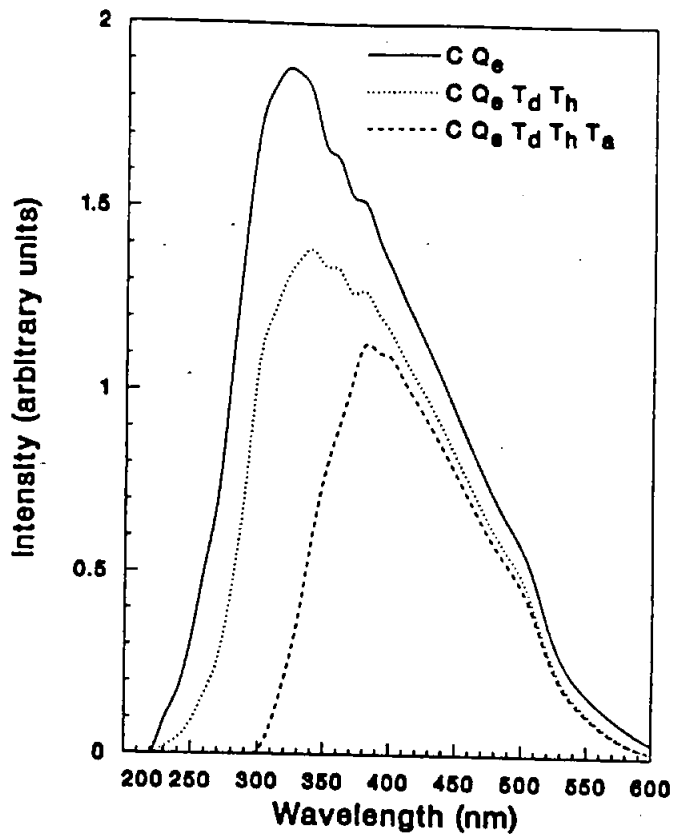


Figure 1

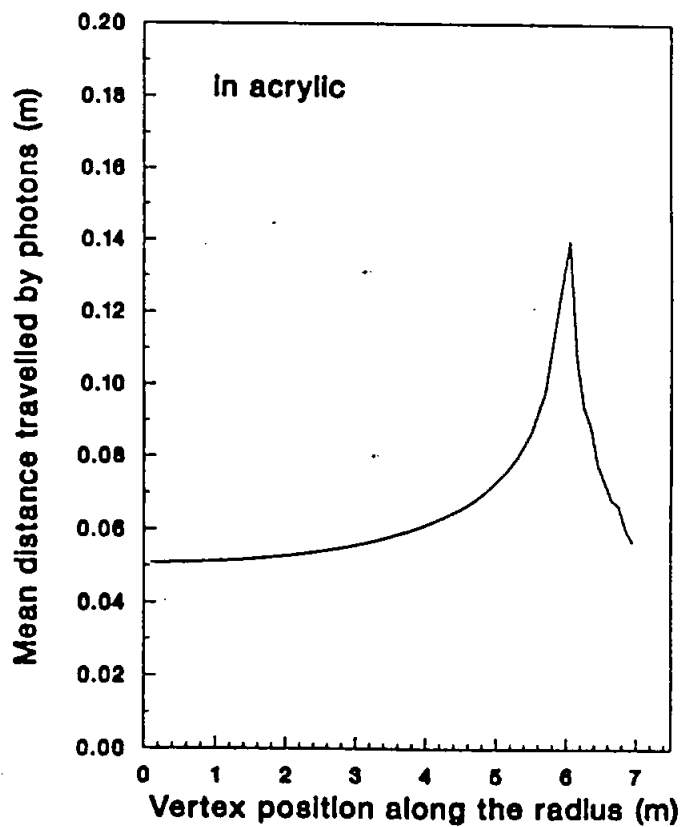


Figure 2

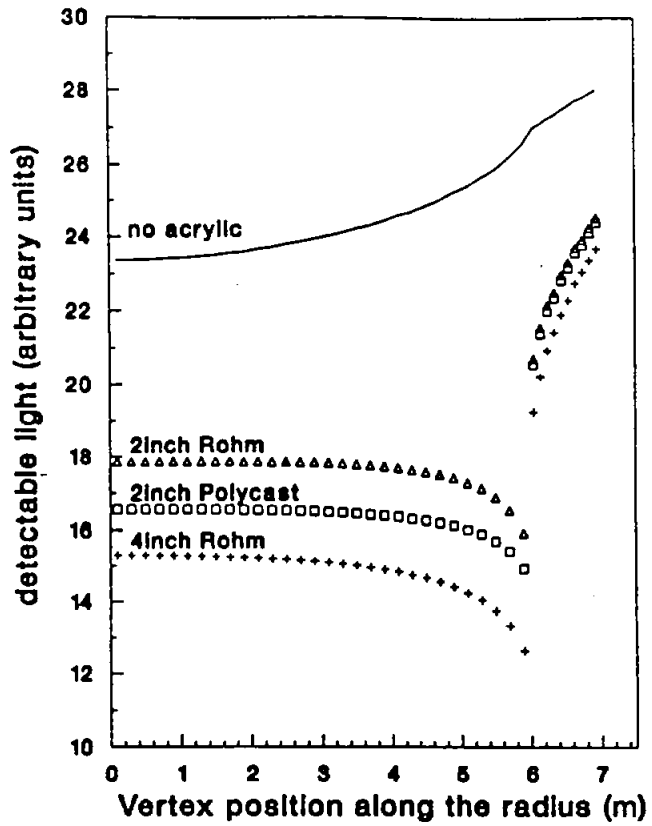


Figure 3

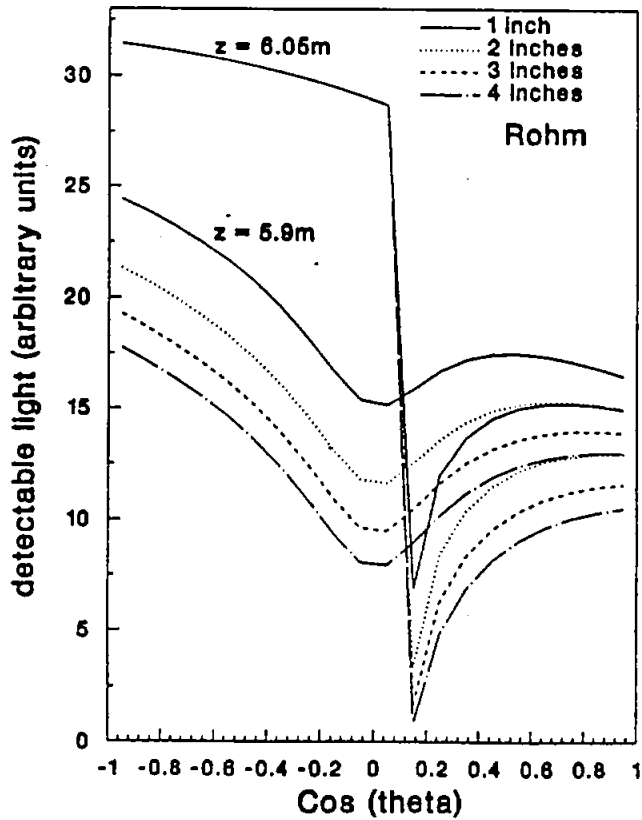


Figure 4